

## FLOOD/DEBRIS FLOW HYDROGRAPH DUE TO COLLAPSE OF A NATURAL DAM BY OVERTOPPING

By

Tamotsu TAKAHASHI

Disaster Prevention Research Institute, Kyoto University, Kyoto, Japan

and

Hajime NAKAGAWA

Disaster Prevention Research Institute, Kyoto University, Kyoto, Japan

### SYNOPSIS

This paper gives a system of equations for the numerical simulation of the failure process of a natural dam due to overtopping. Comparison of the calculated results to those of the flume experiments proves the simulation method is promising for estimating the hydrograph of the resulting flood or debris flow, whose characteristics depend mainly on the surface slope of the dam body as well as the downstream river channel. The sensitivities of some dimensions of the dam in determining the characteristics of the generated flood/debris flow hydrograph are examined by the numerical experiments. The dam height is found to be more effective for determining the peak discharge than the other dimensions such as the size (breadth and depth) of the initially incised channel in the downstream surface of the dam and the channel slope on which the dam is set. So far obtained empirical relationship between the peak discharge of the generated flood and the 'dam factor' is ratified by the numerical simulations.

### INTRODUCTION

Landslides or debris flows sometimes produce the natural dam by blocking the river channel. When the choked ravine is very steep, failure of the dam generates a debris flow and it may result in a severe sediment hazard. A large scale landslide or debris flow can block even a big valley and majority of thus produced natural dams fail catastrophically causing major flooding and loss of life. Mitigation of such kinds of disaster by some structural or nonstructural countermeasures necessitate the knowledges to predict when, where and what characteristic natural dam will be formed, if it may fail, what time is it after formation, and what phenomena will result as the consequence of failure.

As a step to prepare the reply for such requests, this paper presents a mathematical method to predict the discharge hydrograph resulting from failure of the dam due to overtopping under the premise that the topographical conditions of the valley at the place of dam formation, the river discharge and the characteristics of the dam such as size, shape and composing material are known.

### MATHEMATICAL MODELING OF THE PROCESS OF FAILURE

The typical failure processes of the natural dam are classified into three; i.e., the overtopping type, the instantaneous slip failure type and the progressive failure type (1). Among them more than 50 % of the known cases is the overtopping type (2). Because the surface of the natural dam crest is by no means level, the initial overtopping flow may take place from the lowest part in the manner like a miniature debris flow freighting the entrained dam constituting materials and a small stream channel may be trenched on the downstream surface of the dam. The erosion within that incised channel proceeds downward as well as laterally by continuation of overflow, and thus the cross sectional area of the channel increases to increase the water release rate. The increased flow rate, that is the sum of the river's own discharge and the released water discharge from the reservoir, accelerates the erosion and shortly it results

in a catastrophic failure. Thus, the hydrograph of the flood or the debris flow generated by failure of the dam depends on the process of development of the incised channel. Therefore, a quantitative prediction of the hydrograph should simultaneously be the simulation of the process of erosion in the incised channel.

The slope of the incised channel on the dam is diverse from as steep as the angle of repose of the material to a few percents. Therefore, the flow in the channel can be a debris flow in an occasion and a flood flow with some sediment loading in another. Change in slope of that channel can take place even in the process of erosion, so that, the flow equations in the analysis should be applicable to any type of flows. As a debris flow maintains characteristics that are very similar to those of a continuous fluid, a system of momentum and the mass conservation equations for fluid flow are applicable to both of the mere sediment loading flood flow and the debris flow as long as the suitable resistance terms for the respective flows are considered.

Although the flow in the reservoir converging into the lowest part of the dam crest, the enlargement of the incised channel and the deposition of sediments at and downstream of the toe of the dam are the three dimensional phenomena, the characteristic behavior and the approximate quantities of those phenomena may be predicted by the depth-averaged two-dimensional treatment. The depthwise averaged two-dimensional momentum conservation equation for the  $x$ -wise (down valley) direction is

$$\frac{\partial M}{\partial t} + \beta' \frac{\partial(uM)}{\partial x} + \beta'' \frac{\partial(vM)}{\partial y} = gh \sin \theta_{bxo} - gh \cos \theta_{bxo} \frac{\partial(z_b + h)}{\partial x} - \frac{\tau_{bx}}{\rho_T} \quad (1)$$

and for the  $y$ -wise (lateral) direction,

$$\frac{\partial N}{\partial t} + \beta' \frac{\partial(uN)}{\partial x} + \beta'' \frac{\partial(vN)}{\partial y} = gh \sin \theta_{byo} - gh \cos \theta_{byo} \frac{\partial(z_b + h)}{\partial y} - \frac{\tau_{by}}{\rho_T} \quad (2)$$

The continuity equation of the total volume is

$$\frac{\partial h}{\partial t} + \frac{\partial M}{\partial x} + \frac{\partial N}{\partial y} = i\{c_* + (1 - c_*)s_b\} \quad (3)$$

The continuity equation of the particle fraction is

$$\frac{\partial(ch)}{\partial t} + \frac{\partial(cM)}{\partial x} + \frac{\partial(cN)}{\partial y} = ic_* \quad (4)$$

The equation for the bed surface elevation is

$$\frac{\partial z_b}{\partial t} + i = i_{sml} + i_{smr} \quad (5)$$

where  $M = uh$  and  $N = vh$  are the  $x$  and  $y$  components of flow flux;  $u$  and  $v$  are the  $x$  and  $y$  components of mean velocity;  $h$  is the flow depth;  $z_b$  the erosion or deposition thickness measured from the original channel bed elevation;  $\theta_{bxo}$  and  $\theta_{byo}$  are the  $x$  and  $y$  components of the inclination of the original bed surface;  $\rho_T$  is the specific density of the flow,  $\rho_T = c(\sigma - \rho) + \rho$ ;  $c$  the volume concentration of the solids fraction in the flow;  $\sigma$  the density of the solids;  $\rho$  the density of water;  $\beta'$  and  $\beta''$  the momentum coefficients;  $\tau_{bx}$  and  $\tau_{by}$  are the  $x$  and  $y$  components of resistance to flow;  $i$  is the erosion ( $> 0$ ) or the deposition ( $< 0$ ) velocity;  $c_*$  the solids fraction in the bed;  $s_b$  the degree of saturation in the bed (applicable only in cases of erosion, when deposition takes place substitute  $s_b=1$ );  $i_{sml}$  and  $i_{smr}$  are the mean recessing velocity of the left and right hand side banks of the incised channel, respectively;  $t$  the time and  $g$  the acceleration due to gravity.

The resistance to the flow at the bottom  $\tau_{bx}$  and  $\tau_{by}$  in Eqs. 1 and 2 should differently be described corresponding to the respective flow characteristics. According to the so far investigations (1), the following classification of the flow is possible. For the case  $h/d < 30$  ( $d$ : mean particle diameter), the stony-inertial type debris flow in which the laminarly moving particles are dispersed in the entire flow depth appears when the channel slope is steeper than about  $9^\circ$  and/or  $c \geq 0.2$ . If channel slope is flatter than  $9^\circ$  and/or  $c < 0.2$ , the sediment mixture layer can occupy only the lower part of the entire depth of the flow and this type flow is called the immature debris flow. If the slope of the channel is flatter than about  $3^\circ$ , the flow is an ordinary water flow transporting the bed load. For the case  $h/d \geq 30$  and the channel slope is steeper than about  $3^\circ$ , the turbulent muddy flow type debris or immature debris flow appears. When the channel slope is flatter than about  $3^\circ$ , the flow is the ordinary sediment loading water flow. Therefore, if the downstream surface slope of the dam is steeper than  $9^\circ$  and the dam

composing material is coarse the early stage of the overtopping flow may form the stony-inertial debris flow by trenching a self-formed channel and as time goes by with the progress of erosion that channel slope flattens to generate the immature debris flow and then the ordinary flood flow. If the dam is composed of fine materials,  $h/d$  may exceed 30 even in the early stage of overtopping and the turbulent muddy flow may be generated. However, in this paper, only the coarse material case; i.e., at least in the early stage  $h/d$  is assumed to be smaller than 30. The formulae of the resistance to flow in the stony-inertial type debris flow are (1):

$$\tau_{bx} = \frac{\rho T}{8} \left(\frac{d}{h}\right)^2 \frac{u\sqrt{u^2 + v^2}}{\{c + (1-c)\rho/\sigma\}\{(c_*/c)^{1/3} - 1\}^2} \quad (6)$$

$$\tau_{by} = \frac{\rho T}{8} \left(\frac{d}{h}\right)^2 \frac{v\sqrt{u^2 + v^2}}{\{c + (1-c)\rho/\sigma\}\{(c_*/c)^{1/3} - 1\}^2} \quad (7)$$

Those for the immature debris flow are (1):

$$\tau_{bx} = \frac{\rho T}{0.49} \left(\frac{d}{h}\right)^2 u\sqrt{u^2 + v^2}, \quad \tau_{by} = \frac{\rho T}{0.49} \left(\frac{d}{h}\right)^2 v\sqrt{u^2 + v^2} \quad (8), (9)$$

Those for the ordinary sediment laden water flow are:

$$\tau_{bx} = \frac{\rho g n^2 u \sqrt{u^2 + v^2}}{h^{1/3}}, \quad \tau_{by} = \frac{\rho g n^2 v \sqrt{u^2 + v^2}}{h^{1/3}} \quad (10), (11)$$

where  $n$  is the Manning's roughness coefficient.

The bed erosion in the incised channel proceeds under unsaturated bed condition and the tractive force assigned by the interstitial fluid of the overlying sediment-laden flow may be effective. That tractive force;  $\tau_f$ , is the difference between the applied shearing and resisting stresses and for the stony-inertial debris flow and the immature debris flow it is written as:

$$\tau_f = \{(\sigma - \rho)c + \rho\}gh \sin \theta - (\sigma - \rho)ghc \cos \theta R \quad (12)$$

where  $R$  is the dynamic friction coefficient of moving particles on the bed and  $\theta$  is the energy gradient given by

$$\tan \theta = \frac{\sqrt{\tau_{bx}^2 + \tau_{by}^2}}{\rho T g h} \quad (13)$$

Eq. 12 shows the larger the solid concentration in the flow becomes by the erosion and entrainment of the dam composing materials, the smaller the tractive force becomes. When  $c$  attains an equilibrium value;  $c_{eq}$ , no more erosion will take place and at that time  $\tau_f$  is equal to  $\tau_{fe}$ . So far investigations (1) show that the equilibrium concentration for the stony-inertial debris flow is

$$c_{eq} \equiv c_{\infty} = \frac{\rho \tan \theta}{(\sigma - \rho)(\tan \phi - \tan \theta)} \quad (14)$$

where  $\phi$  is the internal friction angle of the bed and  $\tan \phi$  has a value a little larger than  $R$ . The equilibrium concentration for the immature debris flow;  $c_{s\infty}$ , is

$$c_{eq} \equiv c_{s\infty} = 6.7c_{\infty}^2 \quad (15)$$

It should be noted that  $c_{s\infty}$  is less than  $c_{\infty}$ . For the slope on which  $c_{s\infty}$  by Eq. 15 counts less than 0.01,  $c_{eq}$  should be obtained by using an appropriate bed load equation.

The asymptotic behavior of the bed erosion process may be explained by

$$i = K(\tau_{*f} - \tau_{*fe})\sqrt{\frac{\tau_f}{\rho}} \quad (16)$$

where  $K$  is a numerical constant,  $\tau_{*f} = \{\tau_f/[(\sigma - \rho)gd]\}$  and  $\tau_{*fe} = \{\tau_{fe}/[(\sigma - \rho)gd]\}$ , respectively, are the nondimensional tractive force and the nondimensional equilibrium tractive force produced by the interstitial fluid of the flow.

Substitution of Eqs. 12 in which  $\tan \phi$  is used instead of  $R$ , and 14 or 15 or the other  $c_{eq}$  value obtained by a bed load equation into Eq. 16 obtains

$$\frac{i}{\sqrt{gh}} = K \sin^{3/2} \theta \left\{ 1 - \frac{\sigma - \rho}{\rho} c \left( \frac{\tan \phi}{\tan \theta} - 1 \right) \right\}^{1/2} \left( \frac{\tan \phi}{\tan \theta} - 1 \right) (c_{eq} - c) \frac{h}{d} \quad (17)$$

Note that for a bed steeper than the value that satisfies

$$\tan \theta = \frac{c_*(\sigma - \rho)}{c_*(\sigma - \rho) + \rho} \tan \phi \quad (18)$$

the value of  $c_\infty$  from Eq. 14 exceeds  $c_*$ . Because no flow is possible at such a high concentration,  $c$  in Eq. 17 must be replaced by the maximum possible flow concentration, which experimentally is about  $0.9c_*$  (1); consequently,  $i = 0$ .

The velocity,  $u_e$ , that is needed for a debris flow to transport the load by concentration  $c$  neither with erosion nor deposition is given by the equilibrium steady uniform velocity equation obtained from Eqs. 1 and 6

$$u_e = \frac{2}{5d} \left[ \frac{g \sin \theta_e}{0.02} \left\{ c + (1 - c) \frac{\rho}{\sigma} \right\} \right]^{1/2} \left\{ \left( \frac{c_*}{c} \right)^{1/3} - 1 \right\} h^{3/2} \quad (19)$$

where  $\theta_e$  is the slope on which concentration  $c$  is in equilibrium; therefore,  $\tan \theta_e$  is given by substituting  $c$  into  $c_\infty$  in Eq. 14 as following:

$$\tan \theta_e = \frac{c(\sigma - \rho) \tan \phi}{c(\sigma - \rho) + \rho} \quad (20)$$

For the case of the immature debris flow, one obtains from Eq. 15

$$\tan \theta_e = \frac{\sqrt{c}(\sigma - \rho) \tan \phi}{\sqrt{c}(\sigma - \rho) + 2.6\rho} \quad (21)$$

If the flow in the incised channel on the dam body develops to a stony type debris flow while it travels within that channel and then it comes down to the flat area, it begins to decelerate and starts to deposit when the velocity becomes  $pu_e$  ( $p < 1$ ), in which the coefficient  $p$  is introduced to reflect some inertial motion found in the experiment. The amount of the excess particles that should be deposited is  $h(c - c_{eq})$  per unit bed area. Therefore, measuring the time necessary to deposit this amount by  $h/(\delta_d u_e)$ , the equation of deposition rate which takes account such inertial motion may be given by

$$i = \delta_d \left( 1 - \frac{\sqrt{u^2 + v^2}}{pu_e} \right) \frac{c_\infty - c}{c_*} \sqrt{u^2 + v^2} \quad (22)$$

where  $\delta_d$  is a constant and if, in Eq. 22,  $\sqrt{u^2 + v^2} > pu_e$ , one assumes  $i = 0$  no matter what  $i$  is calculated.

If the flow is the immature debris flow or the ordinary water flow, the inertial motion may be neglected and

$$i = \delta_d \frac{c_{eq} - c}{c_*} \sqrt{u^2 + v^2} \quad (23)$$

Lateral erosion velocity is assumed as a function of the shear stress on the side wall assigned by the interstitial fluid of the overlying sediment-laden flow,  $\tau_{sf}$ . The value of  $\tau_{sf}$  is then assumed as one half of the bed shear stress  $\tau_f$ . One may write the recession velocity of the wetted side wall under the surface of the flow  $i_s$  as

$$\frac{i_s}{\sqrt{gh}} = \left( \frac{1}{2} \right)^{3/2} K_s \sin^{3/2} \theta \left\{ 1 - \frac{\sigma - \rho}{\rho} c \left( \frac{\tan \phi}{\tan \theta} - 1 \right) \right\}^{1/2} \left( \frac{\tan \phi}{\tan \theta} - 1 \right) (c_{eq} - c) \frac{h}{d} \quad (24)$$

where  $K_s$  is a constant. By recession of the wetted side wall, the part of the wall above the surface of the flow may lose its stability and fall into the flow. If one assumes the recession of the whole side wall is parallel as shown in Fig. 1, the mean recession velocity of the side walls would be

$$i_{sml} = \frac{h_l}{l_l + h_l} i_{sl}, \quad i_{smr} = \frac{h_r}{l_r + h_r} i_{sr} \quad (25)$$

where  $i_{sml}$  and  $i_{smr}$  are the mean recession velocity at the left and right banks, respectively,  $l_l$  and  $l_r$  are the parts of the left and right banks above the flow surface, respectively.

The finite difference calculation of those system of equations referred to above makes possible to analyse the whole phenomena from the beginning of overtopping to the complete failure of the dam as well as to estimate the time varying quality and quantity of the discharge downstream. However, one should add a special contrivance in the calculation, because on the two dimensional grid system set on the horizontal plane the channel can enlarge its width only discretely in spite of the actual continuous

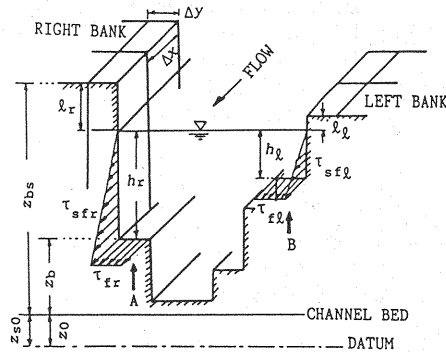


Fig. 1 A cross-section of the incised channel on a dam

widening. To overcome this problem, one may assume that the sediment produced by the recession of banks; e.g.  $i_{smr}(z_{bs} - z_b)\Delta t$ , is supplied only to the cell adjacent to the bank; e.g. cell A in Fig. 1, and it instantaneously raises the elevation of that cell to be eroded by the flow in the channel in the next time step. The channel width is considered not to be changed until the total volume of the sediment supplied, for example, to the cell A becomes equal to the volume of the sediment in the side bank cell at the time of beginning of the side bank erosion;  $t_0$ . At the moment when the two respective volumes of sediment become equal, the channel is considered to be widened by one cell width and the bottom elevation of the new cell adjacent to the new bank is set to be equal to that of the former adjacent cell at time  $t_0$ . The formulation of the procedure is as follows:

$$\int_{t_0}^t i_{sr} h_r \Delta x dt = (z_{bs} + z_{so} - z_b - z_o)|_{t=t_0} \Delta x \Delta y \Rightarrow z_b = z_b|_{t=t_0} \quad (26)$$

## EXPERIMENTS

A steel flume of length 4.97m, width 40cm and depth 20cm was used in the two kinds of experiments. In the first experiment, a 5 cm wide, 2 cm deep and 3 m long channel was incised in the bed adjacent to the transparent flume wall. The bed was composed of the unsaturated sediment mixture whose mean diameter was 1.5 mm. The total width of the bed was 40 cm and the length was equal to that of the incised channel. A wooden weir having the same cross-sectional shape at the crest to the initial bed was installed at the downstream end to avoid erosion from downstream side. The slope of the flume was set to 13°. Steady water flow of 150 cm<sup>3</sup>/sec was introduced from the upstream end. Initially the bed as well as the side bank of the incised channel were covered by a wire net to prevent from erosion before arrival of the flow front at the downstream end. From the instant when the net is removed, changes in vertical as well as lateral erosion rates with time were measured by using the video cameras. Run out water and sediment were separated at the downstream end of the flume and the respective discharges were measured.

In the second experiment, the flume was set at the slope of 3° and a triangular model of the natural dam was installed on the rigid bed. The schematical side view of the set up is shown in Fig. 2. The material of the dam was the sediment mixture whose mean diameter was 2.15mm. The height of the dam was 16cm and the longitudinal base length was 140cm (Case A-1 in Table 1). This corresponds to about 1/250 scale model of the average natural dam in Japan. Water at the flow rate of 100 cm<sup>3</sup>/sec

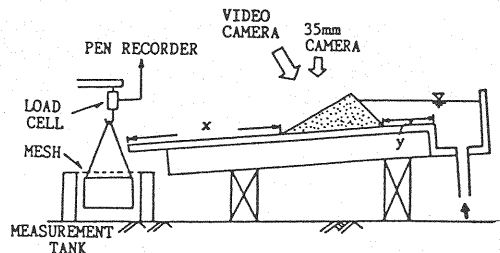


Fig. 2 Experimental set up

was supplied from the upstream end of the flume and in time it overflowed from the notch at the crest of the dam, of which the width was 5cm and the depth was 1.2cm. The overtopping flow incised a channel on the slope of the dam and that channel increased its cross-sectional area with time caused by the sever erosion of released water. Change in the width and bed elevation of the channel were measured by analyses of stereo pair photographs taken in every 5 seconds.

## THE EXPERIMENTAL RESULTS AND THE NUMERICAL SIMULATIONS

The numerical simulations for the cases corresponding the experiments were accomplished using the system of equations stated above. Fig. 3 is a comparison of the results of calculation with the first experiment at the section 220 cm downstream of the inlet. In the calculation following values are used:  $K = 0.06$ ,  $K_s = 1.0$ ,  $\delta_d = 1.0$ ,  $p = 2/3$ ,  $c_* = 0.655$ . Lateral erosion did not necessarily proceed uniformly along the channel, but the sporadic sloughing created discontinuous widenings. The general tendency of widening and vertical erosion of the channel are, however, rather well explained in Fig. 3.

Fig. 4 shows the sediment discharges at the downstream end of the channel in the first experiment. The experimental values fluctuate presumably depending on the local sloughing and other irregularities, but the characteristic sediment yield such as large flow rate at early stage and gradual diminution is explained.

The parameters and the grid systems used in the calculation corresponding the second experiment were  $K = 0.06$ ,  $K_s = 1.0$ ,  $\delta_d = 1.0$ ,  $c_* = 0.655$ ,  $\tan \phi = 0.75$ ,  $\sigma = 2.65 \text{ g/cm}^3$ ,  $d = 2.15 \text{ mm}$ ,  $\Delta x = 10 \text{ cm}$ ,  $\Delta y = 1.25 \text{ cm}$  and  $\Delta t = 0.002 \text{ sec}$ .

Fig. 5 is the bird's-eye view of the process of erosion of the incised channel in the simulation. In the calculation an incised channel of 1cm deep and 5cm wide was set on the entire reach of the downstream side of the dam surface in advance, whereas only a notch at the crest existed in the experiment. Fig. 6 shows the changes of the cross-section of the channel at three points measured downslope from the crest. The instant when the overflow from the crest appeared is defined  $t = 0 \text{ sec}$ . In the early stage the vertical erosion in the calculation is faster than that in the experiment and the calculated channel width is narrower than that in the experiment, but in general the tendency of the channel enlargement is explained. Note that the measurements in the experiments were conducted using a simple stereographer under flowing condition, so that the accuracy is not so good.

The discharge hydrographs obtained in the experiment and by the calculation are compared in Fig. 7. The peak discharge as well as the duration of flood are rather well coincide each other.

The synthetic comparisons of the results of numerical simulation to the results of the two kinds of experiments confirm the presented method of the numerical simulation is valid.

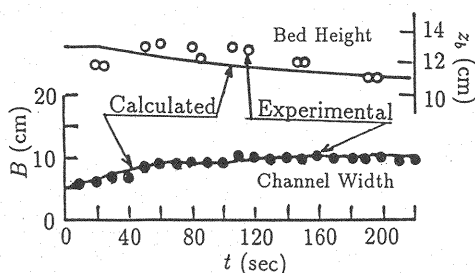


Fig. 3 Variation of the channel width and the bed elevation

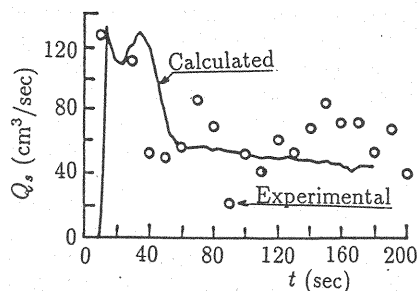


Fig. 4 Sediment discharge at the channel outlet

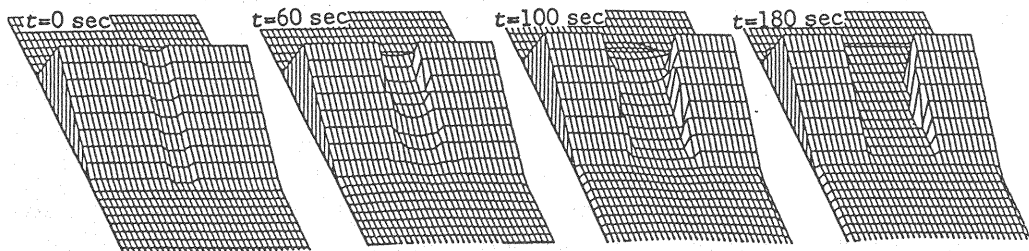


Fig. 5 Process of development of the incised channel

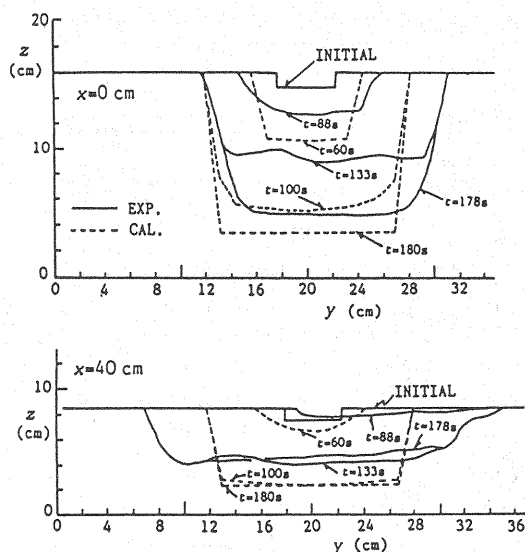


Fig. 6 Cross-sectional shapes of the incised channel at three positions

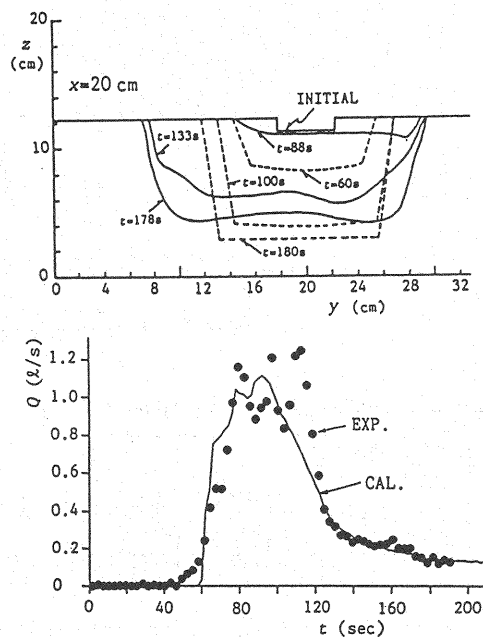


Fig. 7 Discharge hydrographs resulting from failure of the dam

### FACTORS DETERMINING THE PEAK DISCHARGE

Some systematic numerical simulations were conducted to know the dominant factors for determining the peak discharge of the flood/debris flow and to compare the resulting peak flows to the previous empirical data. The first numerical experiments were concerned about the effects of the width and depth of the initial incised channel. The cases examined are listed in Table 1. As far as this examination is concerned, the initial width of the channel little affects the peak discharge and the initial depth of the channel slightly affects in a manner that if it deepens the peak discharge appears earlier (though not specified in the table) and larger. The initial channel size; i.e., the notch size at the crest, however, seems not to be very effective for determining the peak discharge.

In the second numerical experiments, the congruent dams to Case A-1 were set on the different valley slopes as shown by Case B in Table 2. The discharge hydrograph obtained in each case is compared in Fig. 8. Both the peak discharge and the duration of flood/debris flow are larger when the valley slope is flatter.

In the third numerical experiments, the same volume of sediment (volume of landslide to make a dam is the same) made the dams on different valley slopes as shown by Case C in Table 2. The downstream and upstream side slopes of the dam surface, respectively, were kept constant in every cases. Therefore, the height of each dam was different and so was the initial volume of stored water. The resulting peak discharges were also very much different as shown in Table 2. The biggest discharge appeared when the dam was made on flat valley.

The results of the above numerical experiments suggest the most dominant factor to decide the peak discharge is the capacity of the reservoir. If compared under the same water storage capacity, the peak discharge should be larger for the heigher dam, so that as previous investigation correlates, the peak discharge may change depending on the dam factor (dam height  $\times$  water storage capacity). Considering that the numerical experiments correspond to the 1/250 scale model experiments and applying the Froude's similitude, the peak discharges are plotted on the figure obtained by Costa (3) as shown in Fig. 9. One recognizes the peak discharges of the simulations are well correlate to the dam factor and that they have similar tendency to the actual data.

Table 1 Examination of the effect of the incised channel dimension on the peak discharge

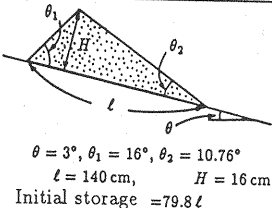
CASE	Channel width (cm)	Channel depth (cm)	Peak discharge ( $\ell/s$ )	Remarks
A-1	5.0	1.0	1.12	
A-2	7.5	1.0	1.13	
A-3	10.0	1.0	1.19	
A-4	5.0	2.0	1.14	
A-5	7.5	2.0	1.20	
A-6	10.0	2.0	1.21	
A-7	5.0	3.0	1.20	
A-8	7.5	3.0	1.20	
A-9	10.0	3.0	1.35	

Table 2 Effect of the valley slope on the peak discharge

CASE	Valley slope (°)	H (cm)	l (cm)	$\theta_1$ (°)	$\theta_2$ (°)	Initial storage ( $\ell$ )	Peak discharge ( $\ell/s$ )
B-1	8	16.0	140	16	10.76	18.6	0.52
B-2	13	16.0	140	16	10.76	4.3	0.26
C-1	1	16.3	137	14	12.76	283.1	2.97
C-2	8	13.4	167	21	5.76	16.2	0.44
C-3	13	5.4	416	26	0.76	1.3	0.12

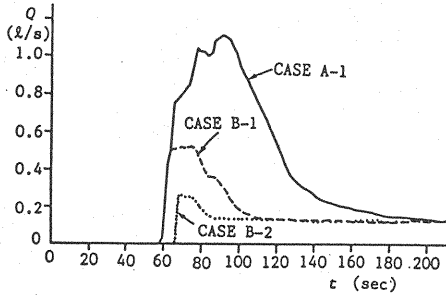


Fig. 8 Discharge hydrographs on various valley slopes

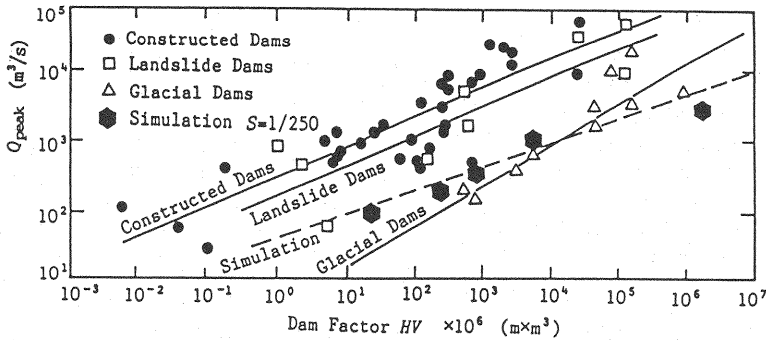


Fig. 9 Dam factor versus peak discharge

CONCLUSION

A system of equations to be used in the numerical simulation of the process of failure of the natural dam due to overtopping and thus to obtain the resulting discharge hydrograph either as a debris flow or an ordinal flood flow was given. Comparison of the calculated results to those of the flume experiments proved the method is promising. Finally, the effects of the size of the initial overtopping stream channel, the dam height, the water storage capacity and the valley slope to the discharge hydrograph are discussed and the peak discharges are discovered to be mostly influenced by the storage capacity of the reservoir and the dam height as previous investigation pointed out.

REFERENCES

1. Takahashi, T. : Debris flow, Monograph Series of IAHR, Balkema, pp.1-165, 1991.



2. Costa, J. E. and R. L. Schuster : The formation and failure of natural dams, Geological Society of America Bulletin, Vol.100, pp.1054-1068, 1988.
3. Costa, J. E. : Floods from dam failures, Flood Geomorphology, pp.439-463, 1988.

## APPENDIX - NOTATION

The following symbols are used in this paper:

$c$	= solids concentration by volume in the flow;
$c_{eq}$	= $c$ in the equilibrium state;
$c_{\infty}, c_{s\infty}$	= equilibrium solids concentration in the stony-inertial and immature debris flows;
$c_*$	= volume concentration of the solids fraction in the bed;
$d$	= representative particle diameter;
$g$	= acceleration due to gravity;
$h$	= depth of the flow;
$i$	= erosion or deposition velocity;
$i_{sml}, i_{smr}$	= mean recessing velocity of the left and right banks;
$K, K_s$	= numerical constants;
$l_l, l_r$	= parts of the left and right banks above the flow surface;
$M, N$	= $x$ and $y$ components of flow flux;
$n$	= Manning's roughness coefficient;
$p$	= numerical constant;
$R$	= dynamic friction coefficient of particles on the bed;
$s_b$	= degree of saturation of the bed;
$t$	= time;
$u, v$	= $x$ and $y$ components of the mean velocity;
$u_e$	= equilibrium velocity of the debris flow;
$x, y$	= coordinate along the valley and lateral to the valley;
$z_b$	= erosion or deposition thickness;
$\beta', \beta''$	= momentum coefficients;
$\delta_d$	= numerical constant;
$\theta$	= gradient of the energy slope;
$\theta_{bxo}, \theta_{byo}$	= $x$ and $y$ components of the inclination of the original bed surface;
$\theta_e$	= slope on which concentration $c$ is in equilibrium;
$\rho$	= density of water;
$\rho_T$	= apparent density of the debris flow;
$\sigma$	= density of solids;
$\tau_{bx}, \tau_{by}$	= $x$ and $y$ components of resistance to flow;
$\tau_f$	= tractive force assigned by the interstitial fluid;
$\tau_{fe}$	= $\tau_f$ in the equilibrium state;
$\tau_{*f}, \tau_{*fe}$	= nondimensional expression of $\tau_f$ and $\tau_{fe}$ ;
$\phi$	= internal friction angle.